GIANTLEAP

DELIVERABLE D4.3

Experiments on Full-Size Stack

PUBLIC

Stefan Hemmer (ElringKlinger), Federico Zenith and
Ivar J. Halvorsen (SINTEF)
Quality Assurance: Frano Barbir (FESB)

GIANTLEAP

Project acronym:	GIANTLEAP
Project title:	Giantleap Improves Automation of Non-polluting Transportation with Lifetime Extension of Automotive PEM fuel cells
Project number:	700101
Document date:	March 30, 2019
Due date:	April 30, 2018
Keywords:	experiments, fuel cell, impedance, shunt, resistor, labview

Abstract: In coordination with task 1.4, ElringKlinger tested the diagnostic approaches for single cells and short stacks developed at FESB on the third full-size stack, to highlight any difference in behaviour and required adjustments to the prognostic approaches. The simple test setup on the full stack test system at ElringKlinger production test lab has provided results that are in line with the expectations for the estimation of the low frequency resistance (LFR). This parameter is related to ageing of the fuel cells, and is intended to be used for prognostics, together with other relevant operational data.

Revision History

Date	Description	Author
Nov 5, 2018	First version LFR tests (Document: D4.3B)	Federico Zenith
Dec 19, 2018	First version deliverable report	Stefan Hemmer
Mar 12, 2019	First draft LFR test results	Ivar Halvorsen
Mar 28, 2019	Input QA	Frano Barbir
Mar 29, 2019	Final Version submitted	Stefan Hemmer
Mar 30, 2019	Minor layout and typo corrections	Federico Zenith

Table of Contents

1 Testing Full-Size Stack Modules

1.1 Motivation

The purpose of this deliverable is to test the diagnostic approaches for single cells and short stacks developed at FESB in work package 1 on the third full-size stack, to highlight any difference in behavior and required adjustments to the prognostic approaches.

1.2 General stack characteristics

Within the GIANTLEAP project ElringKlinger evaluated a new cell configuration for the use a range-extender bus application. As shown in Figure 1, the full-size stack modules were tested mainly at two different pressure levels. At the nominal load point the cell configuration delivers 240 A in atmospheric operation. With pressurized media systems at 1.8 bar_a, the current reaches up 340 A which leads to a power density of 4 kW/L on stack level.

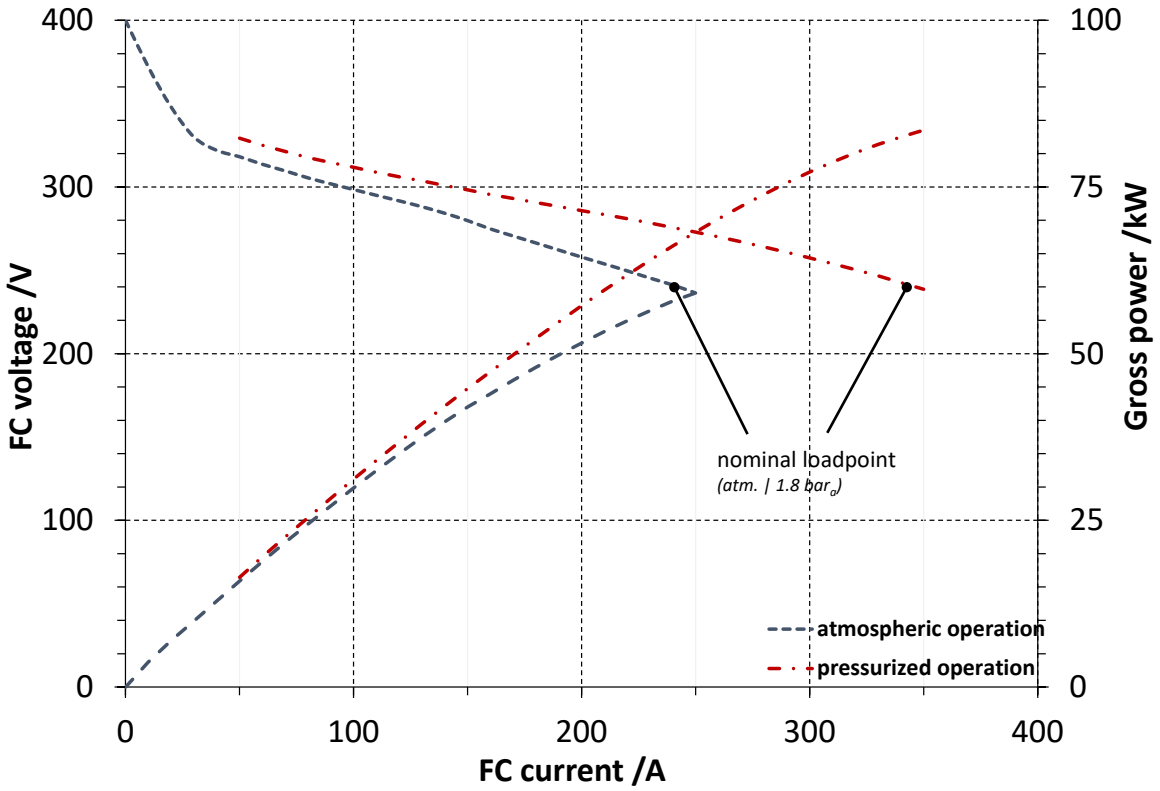

Figure 1: Voltage-Current-Characteristics at different pressure levels / Gross performance of two stack solution

The totally required gross power of the fuel cell stacks calculated by system simulations on the basis of VDL bus drive cycles was set to 80 kW. As the diagram shows, the stacks reach this point at a corresponding voltage of 250 V. The prevailing operating conditions on cathode and cooling side were set in accordance to deliverable D1.2 chapter 4. With regard to the demonstrator bus system, the anode is operated via passive recirculation developed within the GIANTLEAP project. Besides the high performance, the tests showed a very homogeneous cell voltage distribution over the whole load range. This is a strong indication for a well-balanced component selection (bipolar plates, MEA, sealing, etc.) and a robust stack concept.

2 Online diagnostic method: Poor Man's EIS

2.1 Introduction

Pivac et al. (2017, §2.2.3), in GIANTLEAP's deliverable D1.4, identified the EIS spectrum's low-frequency intercept with the real axis (x-axis) as an appropriate prognostic variable to assess the current degradation state of a fuel cell. This point and its change (orange arrow) caused by degradation due to potential cycling is visible in Figure 2 as the rightmost point of all EIS spectra.

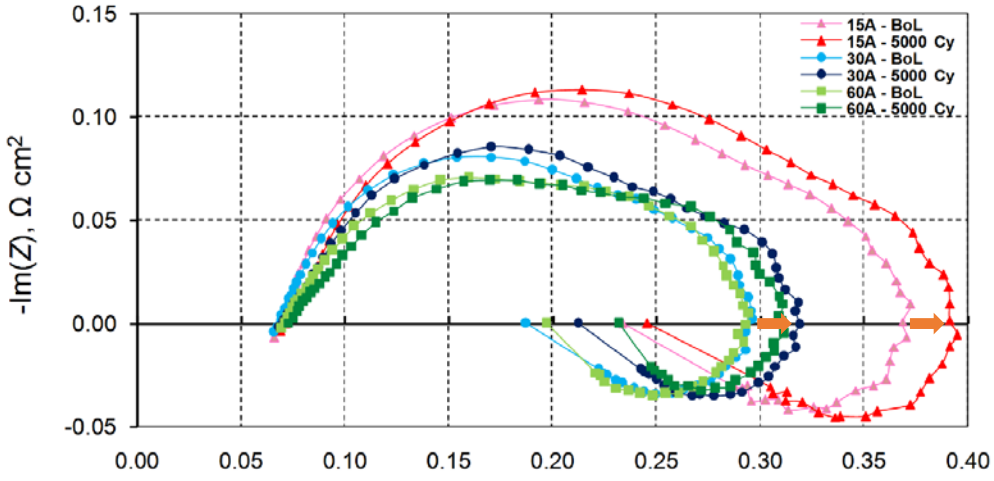

Figure 2: Measured EIS @ BoI vs. 5000 Cycles [D.1.4]

However, measuring a full EIS spectrum with customary EIS sampling equipment is inconvenient, since this equipment is cumbersome, expensive and requires long sampling sessions, often operated by dedicated personnel. An alternative is to focus only on the one point of interest, the low-frequency intercept, and measure it automatically by using a relay feedback.

2.2 Initial testing

As a first step in order to analyse whether ElringKlinger's test bench is capable of running the developed method without changing major components, the following procedure was applied to a full-size stack module:

- Run at constant current until the conditions within the fuel cell are steady. Ensure also that the temperature and pressure are steady
- Run a "square wave" of e.g. [+5A, -5A] for 50 to 60 cycles at a chosen frequency. The amplitude should ideally be "small", but it must be "sufficiently large" to be able to discriminate the corresponding voltage change from the typical noise that can be observed on the voltage measurements
- Record the voltage and current signal with the highest available sampling frequency of the test bench
- In addition to the actual current, also record the command signal to the Load.
- Do the same experiment at some selected frequencies: E.g. [0.1 Hz, 0.2 Hz, 0.5 Hz, 1 Hz]

After 20 minutes the stack reached the steady state point and the load variation was started. As shown in Figure 3 the voltage response to the load variation was measured at all different frequencies. As an example, the enlarged section in the right part of Figure 3 shows the variation in higher resolution.

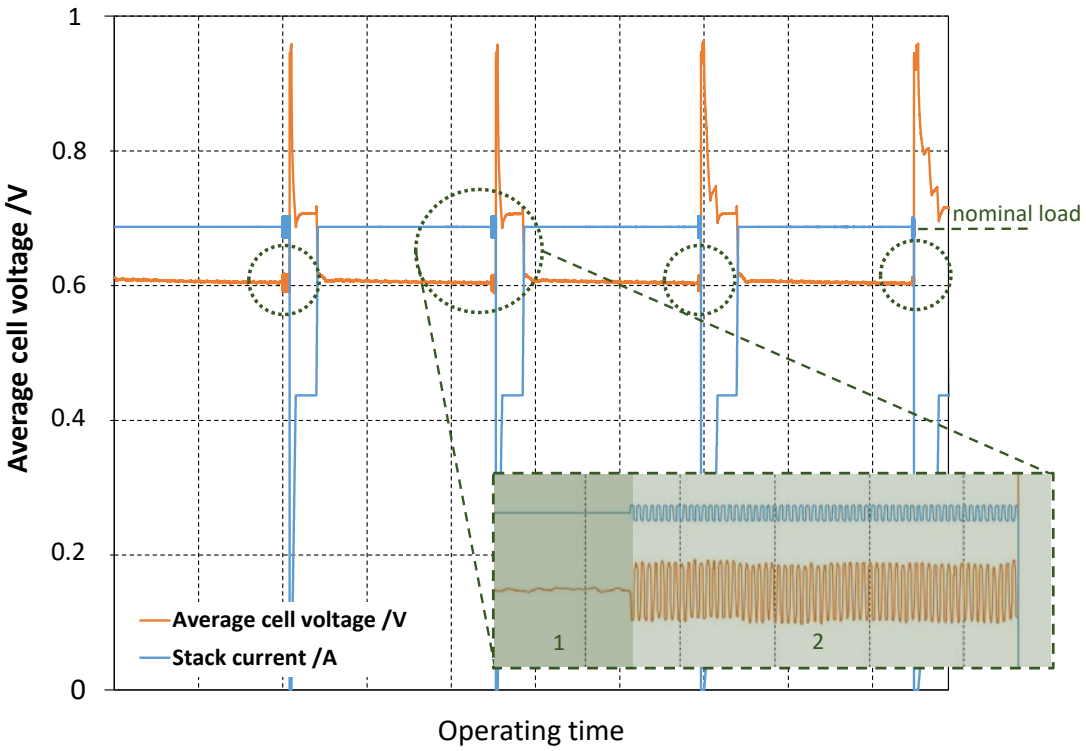

Figure 3: Load variation and voltage response of full-size stack module during pre-testing of POOR Man's EIS method

The difference between the typical voltage noise during operation (1) and the voltage feedback while oscillating the load (2) is clearly visible. Thus the accuracy of the used equipment was confirmed as suitable for the method. After the tests were made, the data was provided to SINTEF in order to analyze the recorded parameters.

2.3 New concept

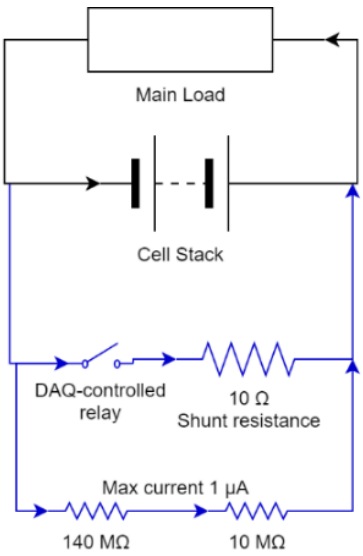

Figure 4: Initial layout for testing of the relay feedback with shunt resistance.

The analysis of the pre-testing data by SINTEF let to the conclusion that the load used by ElringKlinger to test their stacks was too slow in sampling and load changes to be used for a verification of the relay feedback method; furthermore, modifications to the rig to implement the method would have involved expensive consulting fees from the test station's manufacturer. It was therefore suggested to maintain the load in current-setting mode while a shunt resistance would be repeatedly connected and disconnected in parallel to load and stack, in order to oscillate the current passing through the stack. The layout is presented in Figure 5. The shunt resistance would be connected and disconnected by means of a solid-state relay, which are able to operate to a much higher frequency than required. In order to sample the voltage of the stack sufficiently fast, which is necessary to implement the feedback loop, a voltage divider would be added in parallel to the stack, as shown at the bottom of the scheme.

2.4 Implementation of test equipment on EK Test bench

The rig was set up at ElringKlinger's laboratory in Dettingen an der Erms on October 24-25, after the Giantleap project meeting held the two previous day at the same location.

The following additional components were employed for the rig:

- A voltage divider, custom-built by SINTEF, with two resistances sized 1 MΩ and 68 kΩ respectively (lower than the values in Figure 4, as these were readily available standard components). The estimated current through the divider was about 0.1 mA, still well below the expected measurement noise, and therefore still acceptable.
- A TE Connectivity TE1500B10RJ resistor, able to dissipate up to 1.5 kW (Figure 5)
- A Crydom D1D20 DC relay.
- A National Instruments data acquisition unit (DAQ) USB-6002.

Figure 5: Shunt resistor TE1500B10RJ

The following deviations from the original design had to be made in order to complete the tests in the given time:

- The original relay provided by SINTEF was a Crydom D2425, which is an AC model. This was not compatible with a DC load, and a new DC relay was acquired in Stuttgart (the aforementioned D1D20).
- Upon start-up of the rig, the electronic load initiated a shutdown as it had detected an earthing of the stack. Upon analysis it was found that the voltage divider, through the DAQ, its USB cable, the laptop PC used for control and its charging cable, was connected to a power socket's earth. The temporary solution was to run the PC on battery power.

2.5 Execution

Once the rig was able to start, initial tests were run with constant frequencies at multiple values (2 Hz, 1 Hz, 500 mHz, 200 mHz, 100 mHz and 20 mHz). After that, the relay feedback was tested with success.

The relay feedback was implemented in LabVIEW as shown in Figure 6, where the input from the voltage divider is back-calculated to the actual stack voltage, and subtracted from the nominal voltage to obtain the voltage deviation δV. This is integrated twice by two point-by-point integrators, which are initialised to zero value at program start. The integration is weighed by the time interval dt, which is an input to the method. If $\iint \delta V$ is larger than zero, the shunt resistor is connected to the stack.

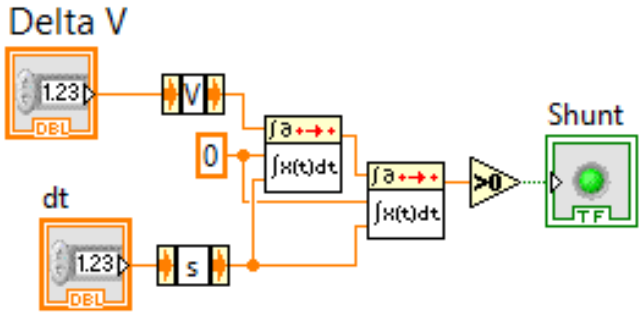

Figure 6: Implementation of the LFR relay feedback in LabVIEW.

The voltage bias estimate is estimated according to the Virtual Instruments diagram shown below in Figure 7.

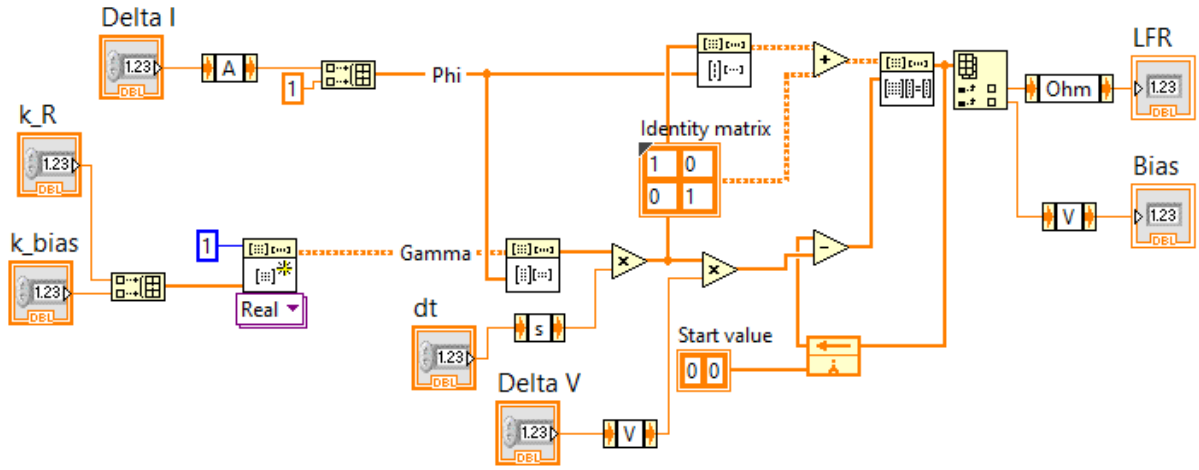

Figure 7: The implicit implementation of the bias and LFR estimator.

Note that Figure 7 does not implement anything different from the algorithm already illustrated in deliverable 3.2, but the implementation relies on an implicit Euler integration, which is less readable than an explicit one. This is chosen because of the stability properties of implicit algorithms, and the experience that an explicit implementation is not numerically stable in LabVIEW. The essential feature for the user is the two tuning parameters k_R and K_bias that can be used for fine tuning of the convergence rate and sensitivity. Note that the bias is applied on line in the algorithm to compensate for slow drift, and the resistance is used in the internal model of the estimator. The resulting LFR estimate for prognostic purpose must be low-pass filtered since there will be a certain cyclic variation during the excitation in the on-line experiment.

2.6 Results

All the tests in the following are carried out in sequence on the same day in 2018. The measurement stack voltage and load system current from ElringKlinger's test system is shown in Figure 8.

Note that the fuel cell current variation does not show up in the lab system since the excitation is carried out by the shunt resistor. The load current disturbance rejection control is so fast that the disturbance, every time the relay is turned on/off, cannot be observed on this current measurement.

Another observation is that there is a slow descending trend on the voltage. This is most likely due to that the excitation is not symmetric around the nominal load current. This can be handled by reducing the load with 50% of the shunt current just before starting cycling, and return afterwards.

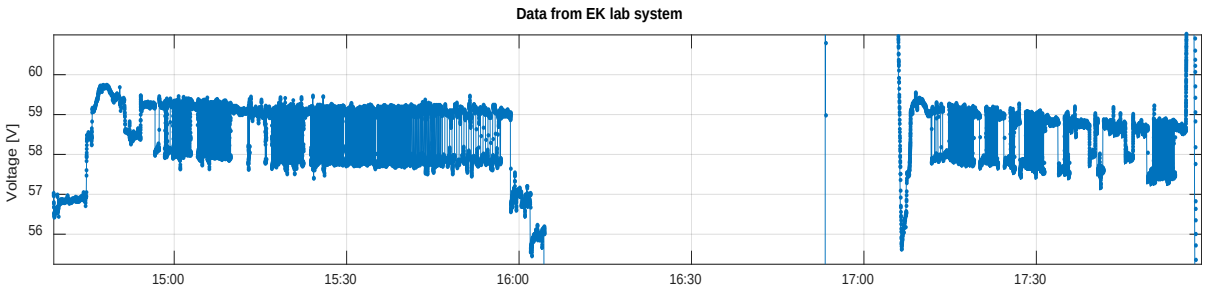

Figure 8: Fuel cell voltage during the test-day. Time units: hour:min

2.6.1 Fixed frequency excitation

The first set of tests applied fixed frequency excitation.

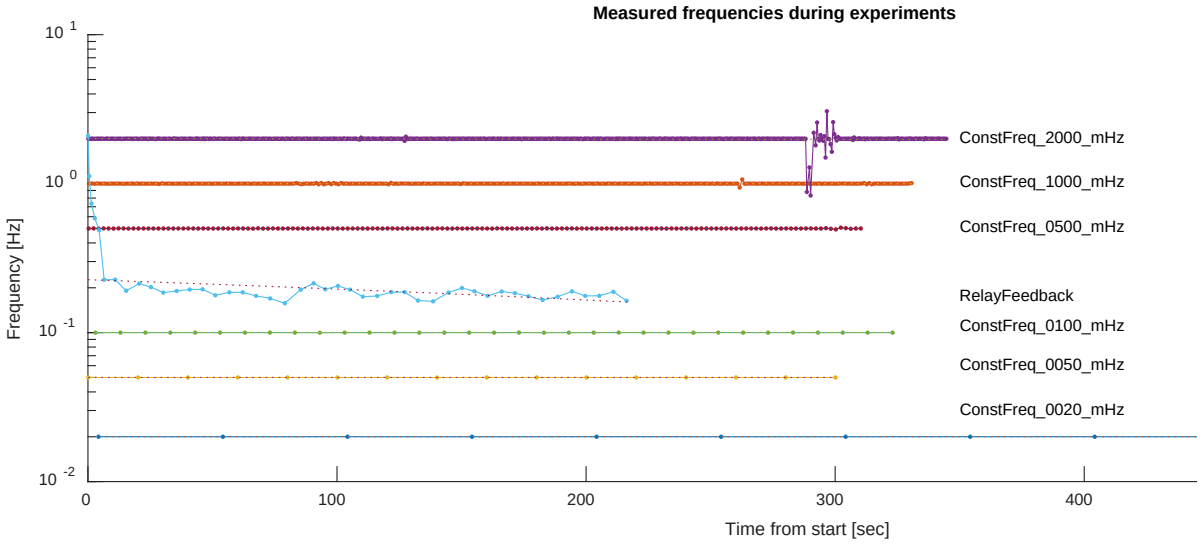

Figure 9: The actual frequencies logged during the tests (logarithmic frequency axis)

By checking the detailed on/off time instants, the frequencies during testing are shown in Figure 9. A small ripple can be observed on the 1 & 2 Hz runs. This is probably due to the LabVIEW PC.

Observe also that the relay feedback frequency rapidly settles to around 220 mHz, but with a descending trend. The relay feedback experiment was carried out from 17:50, and it can be observed that there is an overall descending trend at the time of the test day, so the experiment did not converge completely.

The results from the fixed frequency test at 20mHz (50 second periods) are shown in Figure 10.

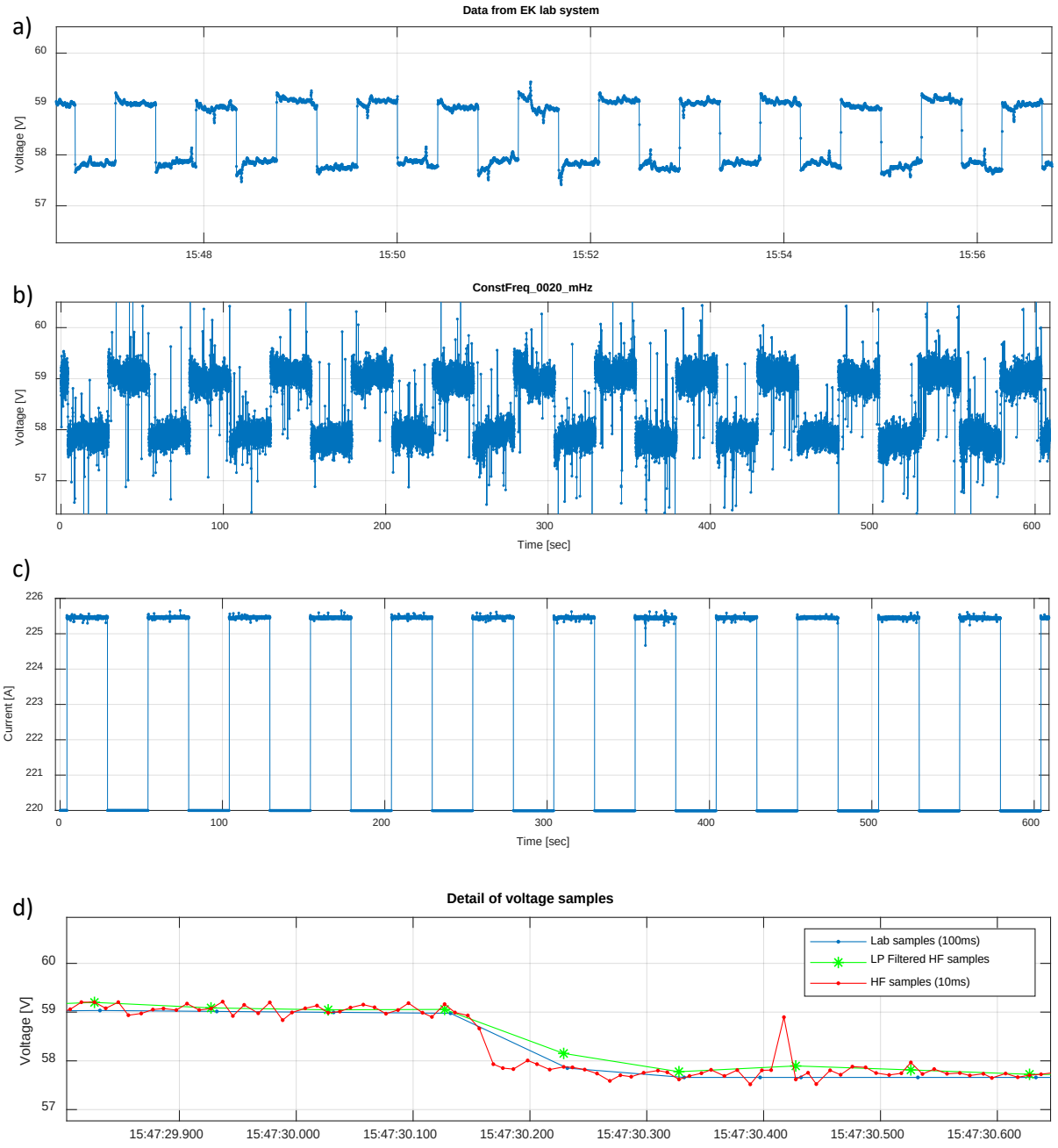

Figure 10: Measured Fuel Cell voltage by the EK lab system (a) and the LabVIEW system (b) and fuel cell current (c), and detail of the voltage measurement in the same axis plus low pass (LP) filtered HF sampled data (d).

The lab system log has a data resolution of 100 ms, while the LabVIEW system samples data every 10 ms. Notice the clearly observable difference in noise level on the two loggings of the same voltage. There are two explanations for this:

1. Unshielded wires and simple ungrounded setup for the data acquisition device of the additional LabVIEW-system, is more exposed for noise than the permanent EK laboratory system instrumentation.
2. The lab system most likely has a low-pass input filter suited for the sample rate, according to Nyquist's sampling theory. (In front of the DAC there shall be a low-pass filter with breakpoint at 2 times the sampling frequency. This is to avoid aliasing of high frequency components in the input signal)

However, one of the important features of the LabVIEW system is the high sampling rate that allows for more precise phase calculation. It is illustrated with filtering the noisy high sample frequency data with a discrete 1st order low-pass filter with 50 ms time constant and resampling from 10 to 100 ms.

That filtered signal becomes quite close to the lab system samples, so this kind of filtering and sampling can explain most of the observed noise.

It is also expected that there may be a small offset deviation since the measurements are done with two independent voltage measurement devices that have not been calibrated versus each other. But from just the visual inspection, the deviation of this kind is small and negligible.

For each case, it is of interest to calculate the gain and phase of the fuel cell impedance. The "gain" is simply the magnitude of the impedance which is a complex number for each frequency. This calculation is carried out by usage of Fourier series analysis. The calculation result can be improved by various filtering techniques and data pre-processing, e.g. wilt point removal. Since this data are to be used for estimating a transfer function point, it is important that the same dynamic filters are applied on both the current signal and the voltage signal to avoid that the phase difference is not affected.

A resulting Fourier series fit of current (inverted) and voltage is shown in Figure 11.

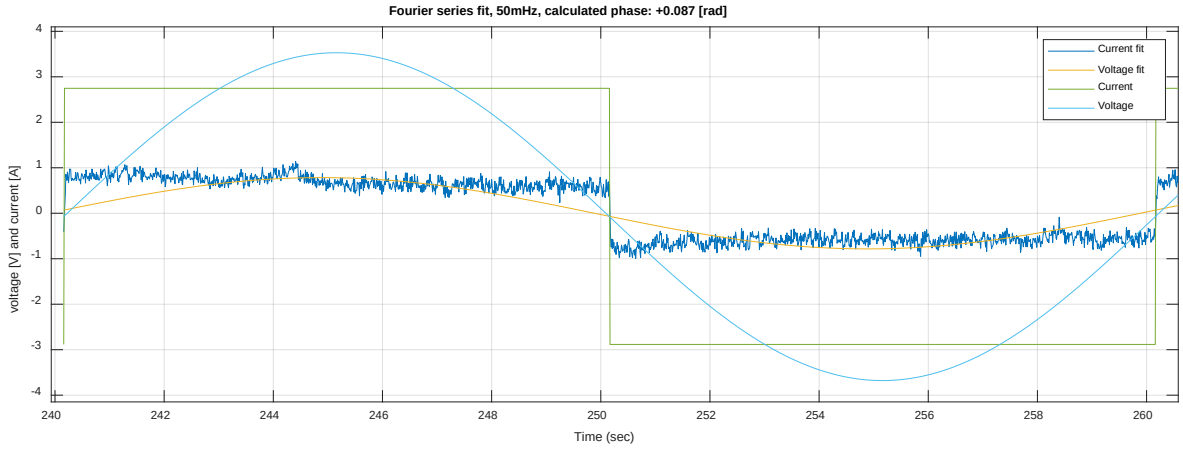

Figure 11: First order harmonic Fourier signal fitted to -current (green) and voltage (noisy blue).

Mean values have been subtracted and voltage and current are plotted with engineering units volt and ampere, respectively. A certain tiny positive phase can be seen at the sine representing the voltage signal compared to the current signal at the zero crossing. This is a low frequency point of 50 mHz, before the Nyquist curve pass through the low frequency intercept point. The absolute value of the impedance is the ratio of amplitudes for the fitted voltage to the fitted current sine signals. This method can be applied for any periodic signal on a linear system.

By putting together all the constant frequency results, a part of a Nyquist plot can be made (Figure 12). Note that the EIS plots usually plot the negative imaginary axis upwards.

A general challenge with this kind of method is that the resulting impedance, as seen from the measurement points, also includes the DC/DC converter. If the DC/DC current control is sufficiently fast, it can be regarded as an "ideal" current source, pulling a constant current from the fuel cell and shunt. Then the observed impedance will be the fuel cell impedance. This seems to be the case for the actual system because no disturbance can be observed on the load current measurement. The sampling rate of 100 ms indicates that the DC/DC is at least faster than that.

The relay excitation is asynchronous with the lab-system sampling rate, so some of the switching instants will occur immediately before the sampling, but still no significant current deviation can be measured on the load, even if the fuel cell current is stepped up and down with steps above 5 A. This indicates that disturbance rejection control of the DC/DC is considerably faster than 100 ms, and even faster than 10 ms.

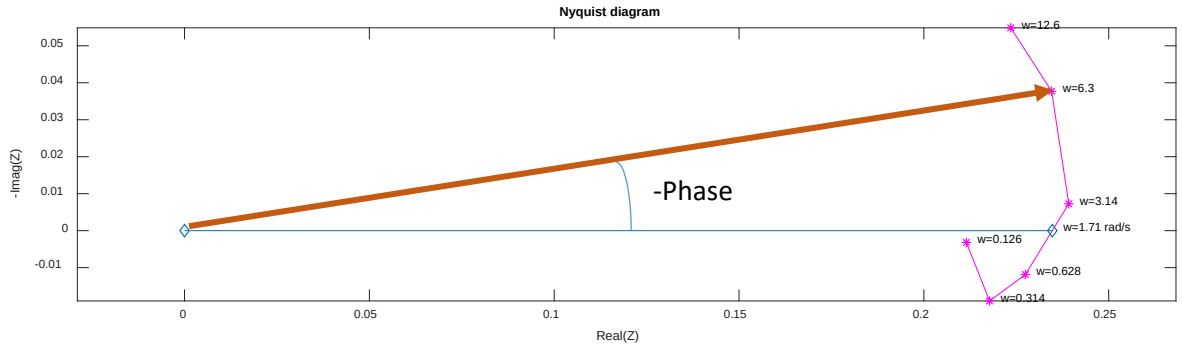

Figure 12: Nyquist diagram points (e.g. a part of EIS) for the results at the constant frequency test. the engineering unit is Ω on both axes.

From this Nyquist diagram shown in Figure 12 it is possible to interpolate the LFR frequency . From theoretical analysis of a fuel cell impedance model, the phase has close to linear relationship to the logarithmic frequency in the region around the LFR point. The resulting LFR frequency estimate based on this is **1.71 rad/s = 0.27 Hz**.

Similarly, the LFR resistance can be estimated by the same procedure to R = 0.23 Ω.

However, observe from the diagram that the Nyquist curve seems to have certain slope through the LFR point by this simple approximation. The real Nyquist curve between the neighbouring points is not a straight line. So, the maximum point R = 0.24 Ω may be a better also a reasonable estimate.

2.6.2 Relay feedback excitation

A single relay excitation experiment was carried out. The development of the frequency can be seen in Figure 13. The oscillations are fast in the beginning, converging fast to a reasonable range. However, in this experiment the frequency does not settle completely as shown in Figure 9.

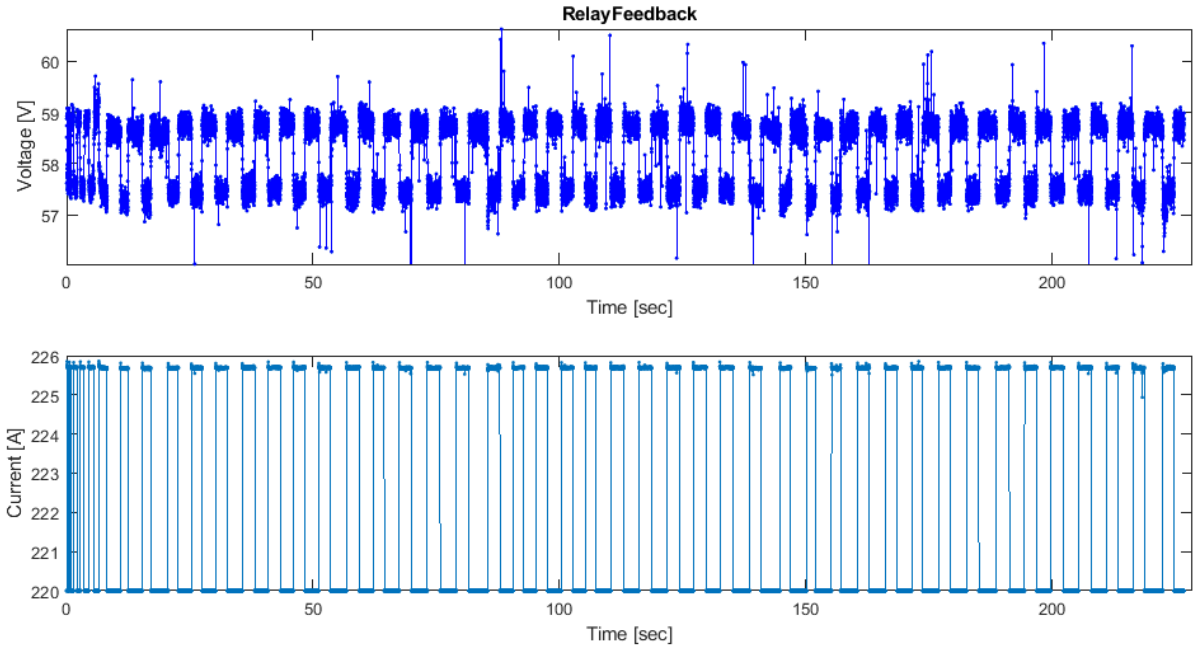

Figure 13: Voltage and current measurements as function of time [seconds] during the relay feedback experiment.

The directly estimated values of bias and resistance are shown in Figure 14. These are unfiltered and are given directly from the LabVIEW algorithm.

The bias estimate is close to a ramp and have not settled. This is due to the overall decreasing trend of the voltage excitation as can be observed in Figure 8.

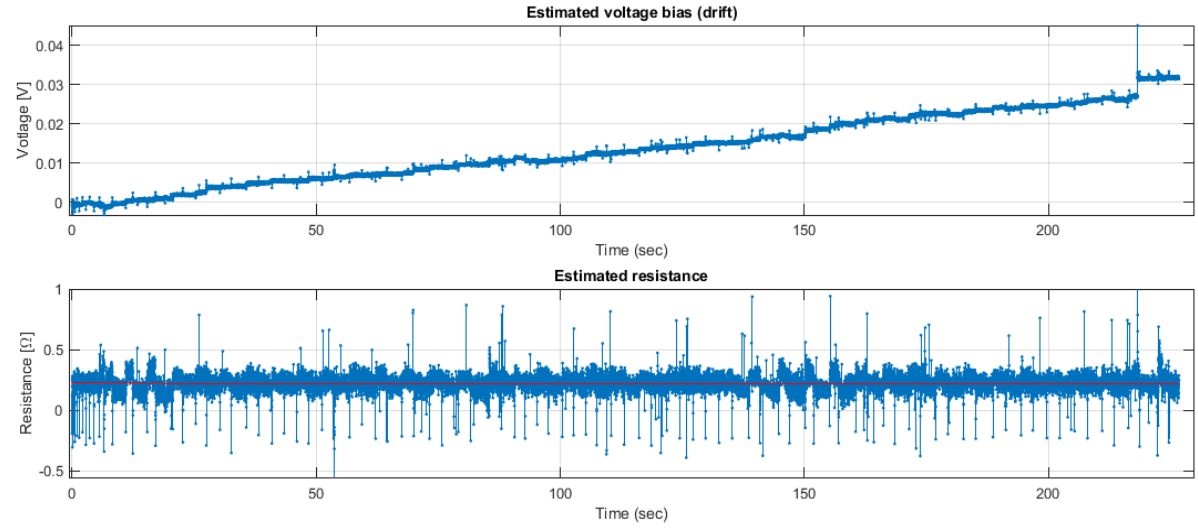

Figure 14: Estimated voltage bias and resistance. Low-pass filtered resistance estimate is shown in red.

The resistance estimate has to be filtered, and a low-pass filtered signal is shown on the noisier estimate (filter time constant is 60 seconds). The end value of the filter is 0.224 Ω.

Another approach is to filter both current and signal with a band-pass filter with a central frequency close to the actual oscillating frequency (around 200 mHz = 1.26 rad/s). Then simply apply least square fit of the filtered data. The resulting resistance estimate is 0.230 Ω. This is also close to the estimated value obtained from the constant frequency estimations.

Being a first full test for the relay excitation algorithm on the full stack, the result must be said to be positive. The most important is that the algorithm is stable and fast.

A lesson learned is to ensure that it would be desirable to carry out the current excitation around the steady value before start of the excitation.

The estimates and the convergence rate of the algorithm can be improved by adjusting the parameters of the algorithm itself, and on signal postprocessing.

The background for the setup with an extra shunt resistor (Figure 4) was used since the load control current setpoint could not be changed as rapid as desired in the feedback. Using the shunt, was a quick workaround such that no modifications was needed on the lab system's load control functionality.

The disturbance rejection capabilities of the DC/DC are more than fast enough, and it will most likely be possible to introduce a current setpoint step with the same quick response as for the disturbance rejection. This will require some low-level updates of the lab power control system and was not possible in time for this kind of testing. In addition, the data log system with a faster sampling rate was also needed. So, the simple add-on LabView system and the physical relay and shunt resistor could do the job.

In practical implementation within a system, the relay excitation method does require a fast sampling rate for execution but does really not rely on the same fast datalogging sampling frequency. In the Giantleap pilot, the control system from BEG has sufficient fast sampling rate for this implementation. Then the "relay" is implemented in software and its output is the setpoint change to the load control DC/DC unit.

3 Conclusions

The simple test setup on the full stack test system at ElringKlinger production test lab has provided results that are in line with the expectations for the estimation the low frequency resistance (LFR). This parameter is related to ageing of the fuel cells, and is intended to be used for prognostics, together with other relevant operational data.

An implementation in a fuel cell system like the Giantleap-pilot is possible. In that case, without the physical relay and shunt used in this test, but with a "software relay" that perturbs the DC/DC load control setpoint.